Journal of Photochemistry and Photobiology A: Chemistry 200 (2008) 270–276

Contents lists available at ScienceDirect

Journal of Photochemistry and Photobiology A: Chemistry

journal homepage: www.elsevier.com/locate/jphotochem

Photoinduced electron transfer between quinones and amines in micellar media: Tuning the Marcus inversion region

Ashis Kumar Satpati [a], Manoj Kumbhakar [b,*], Sukhendu Nath [b], Haridas Pal [b,*]

[a] Analytical Chemistry Division, Bhabha Atomic Research Centre, Trombay, Mumbai 400085, Maharashtra, India
[b] Radiation & Photochemistry Division, Bhabha Atomic Research Centre, Trombay, Mumbai 400085, Maharashtra, India

ARTICLE INFO

Article history:
Received 17 April 2008
Received in revised form 25 July 2008
Accepted 6 August 2008
Available online 14 August 2008

Keywords:
Micellar electron transfer
Triton-X-100
Brij-35
Cetyltrimethylammonium bromide
Marcus inversion
Quinone

ABSTRACT

Electron transfer (ET) rates between quinone acceptors and amine donors in micellar media show Marcus inversion behavior on correlating with the free energy changes of the ET reactions. The onset of Marcus inversion in these systems is seen to be tuned by about 0.25 eV by changing the type of the micelle. The results are rationalized on the basis of two-dimensional ET theory where ET occurs along intramolecular coordinate with non-equilibrium configuration along solvation coordinate. Maximum ET rates are seen to vary by about one order of magnitude in different micelles, and are attributed to the micelle-dependent changes in the separations of the interacting quinone–amine pairs. Tunings of Marcus inversion and ET rates by changing micellar microenvironments have been observed and suggested to have useful implications in different applied areas.

1. Introduction

Photoinduced electron transfer (ET) in confined media is an important research topic for quite sometime [1–10]. The influence of micro-heterogeneous media on the energetics and dynamics of intermolecular ET reactions has been investigated quite extensively in recent years by our group [11–17] including others [18–24]. In confined media, like micelles and reverse micelles, favorable modification of reaction parameters, especially the reduction in the effective reorganization energy and the retardation of the reactant diffusion, are understood to assist the easy observation of Marcus inversion behavior for bimolecular ET reactions [11–22], which is otherwise normally obscured for such reactions in homogeneous solution [25–29].

Following Marcus ET theory, the rate constant k_{et} for ET reaction is expressed as [28]

$$k_{et} = \frac{2\pi V_{el}^2}{\hbar}(4\pi\lambda k_B T)^{-1/2} \exp\left\{-\frac{(\Delta G^\circ + \lambda)^2}{4\lambda k_B T}\right\} \quad (1)$$

where V_{el} is the electronic coupling matrix element, λ is the total reorganization energy (sum of intramolecular (λ_i) and solvent reorganization (λ_s) contributions), k_B is the Boltzman constant, T is the absolute temperature and ΔG° is the free energy change for the ET reaction. As can be realized from Eq. (1), with V_{el} unchanged (a reasonably valid assumption for the ET systems involving homologous series of donors and/or acceptors), the value of k_{et} should follow a bell-shaped behavior with the exergonicity ($-\Delta G^\circ$) of the reaction. Thus, the value of k_{et} should initially increase with the reaction exergonicity as long as $-\Delta G^\circ < \lambda$. This exergonicity region is commonly known as the normal Marcus region and often encountered in the ET reactions. As the reaction exergonicity becomes equal to λ, i.e. $-\Delta G^\circ = \lambda$, the rate constant k_{et} attends its maximum value. This unique situation is known as the Marcus barrierless condition for the ET reaction. The most interesting feature arises when the exergonicity for the ET reaction increases beyond λ. For this exergonicity region, where $-\Delta G^\circ > \lambda$, Eq. (1) suggests that the ET rate constant should decrease gradually with the increasing exergonocity. This distinctive feature is universally known as the Marcus inversion and the corresponding exergonicity region is called the Marcus inversion region. Needles to mention that the predicted inversion of the ET rates at the higher exergonicity region ($-\Delta G^\circ > \lambda$) is the most stimulating aspect of the Marcus ET theory and attracted the attention of many researchers to investigate, understand and demonstrate the details of this aspect for many years [1–29].

Relevance of Marcus inversion can be easily perceived while considering the efficiency of a photoinduced ET (PET) process where an energy wasting reverse ET (producing ground state reactant back) is also associated to the system. Invariably, the reverse

* Corresponding authors. Fax: +91 22 25505151/19613.
E-mail addresses: manojk@barc.gov.in (M. Kumbhakar), hpal@barc.gov.in (H. Pal).

1010-6030/$ – see front matter © 2008 Elsevier B.V. All rights reserved.
doi:10.1016/j.jphotochem.2008.08.001

ET occurs at a higher exergonicity than the forward PET reaction [28]. For a useful PET system, the important criterion is that the forward ET should be faster than the reverse ET. This can be easily achieved if the reverse ET is made to occur in the inversion region. In fact, this is the condition that nature utilizes in photosynthesis to maximize the charge separation efficiency [28]. Thus, it is evident that the understanding of the ET system, especially the nature of the Marcus correlation curve, is an important aspect in designing a PET system for a useful application.

In this paper PET results of different anthraquinone–aromatic amine systems in triton-X-100 (TX100), brij-35 (BJ35) and cetyltrimethylammonium bromide (CTAB) micellar solutions have been presented with an aim to understand the possible tunability of Marcus correlation curves for the ET reactions by changing the characteristics of the microheterogeneous media. Results for the similar quinone–amine systems reported earlier by us in sodium dodecyl sulphate (SDS) micellar solutions [13] have also been reconsidered in the present study for a comparison with the results in TX100, BJ35 and CTAB micelles.

2. Experimental

TX100 (Sigma), BJ35 (Pierce Chemical Co.) and CTAB (Hopkin and Williams) were used as-received. The electron acceptors, namely, 1,4-dihydroxy-9,10-anthraquinone (DHAQ), 1-amino-4-hydroxy-9,10-anthraquinone (AHAQ), and 1,4-diamino-9,10-anthraquinone (DAAQ), were obtained either from Aldrich, USA, or TCI, Japan, and purified by repeated crystallization from methanol (DHAQ) or cyclohexane (AHAQ and DAAQ). The acceptor 2-hydroxy-9,10-anthraquinone (HAQ) was synthesized from 2-aminoanthraquinone (TCI, Japan) by diazotization followed by hydrolysis in hot acidic water and purified by repeated crystallization from methanol. The donors, namely, *N*,*N*-dimethylaniline (DMAN), *N*,*N*-diethylaniline (DEAN), and *N*,*N*-dimethyl-*p*-toluidine (DMPT), were obtained from Spectrochem (India) or Qualigens Fine Chemicals (India) and were purified by vacuum distillation just before use. The chemical structures of the quinones and amines used in this study are given in Scheme 1.

In experimental solutions, TX100 and BJ35 micelle concentrations were ~1 mM whereas CTAB micelle concentration was ~0.2 mM (because of lower solubility). The micellar concentration was estimated from the knowledge of the surfactant concentration used and the values of their CMC and aggregation numbers. Quinone concentrations used were ~10 μM, such that not more than one acceptor molecule can occupy a single micelle. Amine concentrations used were always higher than the micelle concentrations, and varied over a wide range. Effective concentrations ($[Q]_{eff}$) of the amines in the micelles were calculated as in our earlier studies considering that the amines mainly reside in the hydrated Corona region of the micelles [11–16]. Though this method of calculating $[Q]_{eff}$ can lead to some over- or under-estimation in the values obtained depending on the errors associated with the micellar dimensions used, this should not affect the nature of the Marcus correlation curve in a particular micelle, as all the amines used are of similar nature. Such a consideration for $[Q]_{eff}$ has been applied quite extensively by many other groups in studying fluorescence quenching process in micellar media [18–22,30].

JASCO UV–vis spectrophotometer (V-530) and Hitachi spectrofluorimeter (F-4010) were used for absorption and fluorescence spectral measurements. A time-correlated single-photon-counting (TCSPC) spectrometer from IBH, UK, was used to measure fluorescence decays, using either 560 or 373 nm LEDs as the excitation sources. Instrument response function (IRF) for this setup is ~1.2 ns at FWHM. The reduction potentials of the quinone derivatives ($E(Q/Q^-)$) in micellar solutions were measured by cyclic voltammetric (CV) method using an Eco-Chemie Potentiostat/Galvanostat-100, with a GPES 4.9 software. Micellar solutions of quinones containing supporting electrolyte (0.1 mol dm^{-3} KCl) were first de-aerated by purging high-purity N_2 gas for about 10 min. CV measurements were then carried out using hanging mercury drop as the working electrode, graphite rod as the counter electrode and saturated calomel electrode (SCE) as the reference electrode. The oxidation potentials of the amines ($E(A/A^+)$) in micellar solutions were estimated using glassy carbon as the working electrode. In the present study all the absorption, fluorescence and CV measurements were carried out at ambient temperature (25 ± 1 °C). Various energy parameters of the donors and acceptors used in the present study in TX100, BJ35 and CTAB micelles are listed in Table 1. In the present work we would also compare the ET results in the above three micelles with those obtained earlier in our studies in SDS micellar solutions [13]. Thus, various energy parameters of the donors and acceptors in SDS micelle are also listed in Table 1.

3. Results and discussion

In micellar solutions the quinones show largely enhanced solubility in comparison to their solubility in bulk water. Considering the polar nature of the quinones, they are expected to be solubilized preferentially in the hydrated corona region of the micelles than in the nonpolar micellar core. In all the three micelles, even in the presence of very high-amine concentrations there is no change in

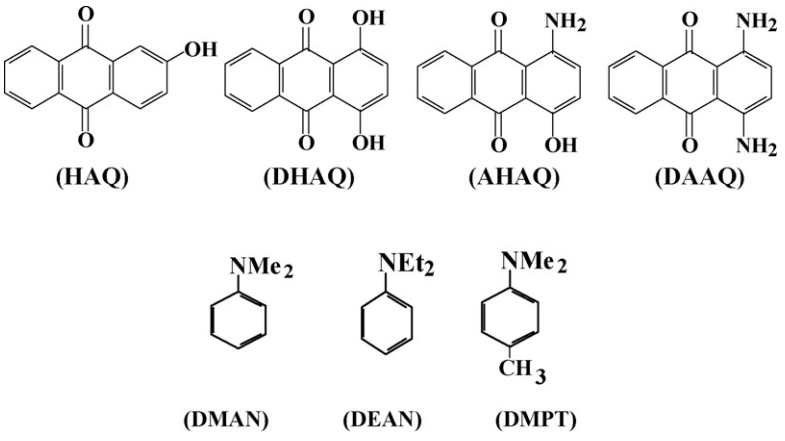

Scheme 1. Chemical structures of the quinones and amines used in the present study.

Table 1
Redox potentials and E_{00} values for the quinones and amine systems in TX100, BJ35 CTAB and SDS micellar solutions

Acceptors	E^{q}_{00} (eV)				$E(Q/Q^{-})$ (V)			
	TX100	BJ35	CTAB	SDS[a]	TX100	BJ35	CTAB	SDS[a]
(A) Parameters for quinines								
DAAQ	2.16	2.10	2.12	2.04	−1.30	−1.01	−1.13	−1.280
AHAQ	2.10	2.11	2.10	2.11	−1.29	−0.97	−1.15	−1.275
DHAQ	2.38	2.37	2.37	2.36	−1.26	−0.96	−1.13	−1.270
HAQ	3.06	3.08	3.06	3.12	−1.25	−0.96	−1.14	−1.230

Donors	E^{am}_{00} (eV)[b]	$E(A/A^{+})$ (V)			
		TX100	BJ35	CTAB	SDS[a]
(B) Parameters for amines					
DMAN	3.81	0.63	0.70	0.65	0.59
DEAN	3.77	0.59	0.68	0.63	0.55
DMPT	3.60	0.53	0.62	0.57	0.53

[a] The values for the parameters in SDS were taken from Ref. [13].
[b] The E^{am}_{00} values are in accetonitrile solution as reported in Ref. [26].

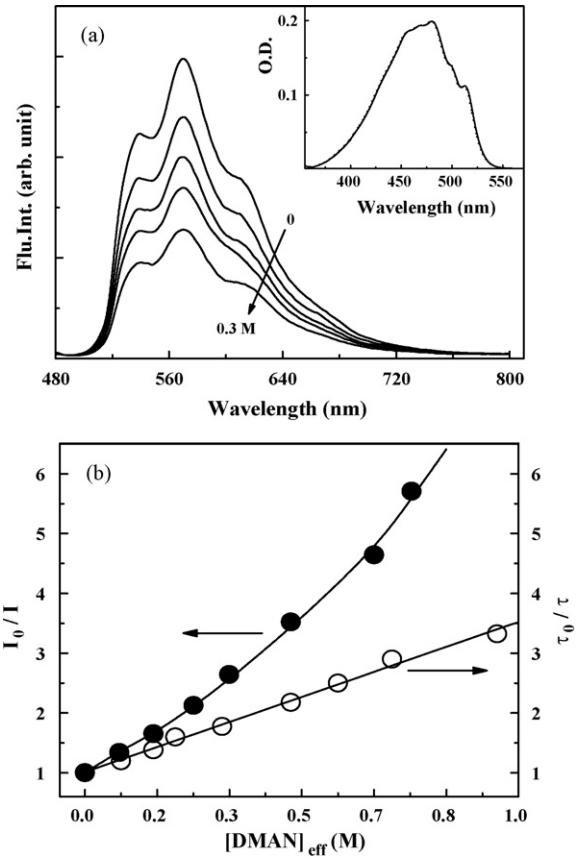

Fig. 1. (a) SS fluorescence spectra of DHAQ in CTAB micelle at different effective concentration of DMAN. (Inset) Absorption spectra of DHAQ in absence (solid line) and presence (dashed line) of DMAN ($[Q]_{eff}$ = 0.75 M) in CTAB micelle. (b) SV plots from SS (●) and TR (○) fluorescence quenching of DHAQ by DMAN in CTAB micelle.

the absorption spectra of the quinones, suggesting no ground state complex formation in the present systems [25]. Fluorescence intensity of the quinones in all the micelles undergo strong quenching on addition of the amines, without any observable change in the spectral shape, suggesting no exciplex formation in these systems [25]. Stern–Volmer (SV) plots [25] for the steady-state (SS) fluorescence quenching always show a positive deviation from linearity at higher amine concentrations, suggesting the presence of reasonable static/ultrafast quenching contributions, possibly arising due to the fraction of the close-contact quinone–amine pairs at higher amine concentrations, as suggested earlier [11–16,25]. Typical SS quenching and SV plots for DHAQ-DMAN system in CTAB micelle are shown in Fig. 1(a) and (b), respectively. Since the SS quenching always indicates the presence of static-quenching contribution, the quenching constants (k_q^{TR}) for the present systems were in fact estimated from the time-resolved (TR) measurements, discussed below.

In TR studies, fluorescence decays of the quinones in TX100, BJ35 and CTAB micelles were measured at different amine concentrations. Though the decays were effectively single exponential in the absence of the amines, they showed clear non-single-exponential behavior in the presence of the amines. Typical results with TR fluorescence quenching measurements for DHAQ-DMAN and HAQ-DMAN systems in CTAB micellar solutions are shown in Fig. 2(a) and (b), respectively. As will be discussed latter, the DHAQ-DMAN system falls closer to the maxima and HAQ-DMAN system falls in the inversion region of the Marcus correlation curve in CTAB micellar solution.

As discussed in our earlier studies [11–16], quenching process in micellar media effectively occurs under nondiffusive condition (quenching constant k_q > the diffusional rate constant, k_d) and thus the reaction kinetics in these systems is mainly determined by the distant-dependent distribution $g(r)$ of the quenchers around a fluorophore [3–6]. In this situation, since ET rate would be distance dependent, it introduces an inherent non-single exponential nature of the fluorescence decays in the presence of quenchers, as discussed in our earlier works [11–16]. For the present systems with TCSPC measurements, due to limited time resolution of the instrument (IRF ~1.2 ns), it is evident that the instantaneous/static part of the quenching process arising due to the fraction of the close-contact quinone–amine pairs [11–16] will not be observed. However, the dynamics of the nanosecond/sub-nanosecond quenching components, which arise due to the fraction of the quinone–amine pairs that are not in direct contact, are expected to be well observed in the fluorescence decays measured by TCSPC instrument. In the present paper, thus, all our discussion is based on this nanosecond/sub-nanosecond quenching components. As the observed fluorescence decays in the presence of the amines were non-single-exponential, and since the estimation of the function $g(r)$ for the amines in a micelle is an extremely difficult task, we have adopted a simple approach of analyzing the fluorescence decays to effectively obtain the average quenching kinetics based on the estimation of the average fluorescence lifetimes (τ_{av}) of quinones in the presence of the quenchers [11–16,18–22]. By definition average lifetime should be expressed as

$$\tau_{av} \approx \frac{\int_0^\infty tI(t)\,dt}{\int_0^\infty I(t)\,dt} \quad (2)$$

For the present systems it is seen that the fluorescence decays are reasonably fitted with a bi-exponential function even in the presence of the highest amine concentration used. Thus, assuming $I(t)$ to be bi-exponential in nature, Eq. (2) can be simplified to express τ_{av} as

$$\tau_{av} = a_1\tau_1 + a_2\tau_2 \quad (3)$$

where τ_1 and τ_2 are the two fluorescence lifetimes and a_1 and a_2 are their relative contributions. It is seen that in all the micellar solution the τ_{av} values for the quinones gradually decrease with an increase in the amine concentration in the solution. The τ_{av} values obtained at different amine concentrations were then utilized to estimate the k_q^{TR} values for the present systems using the SV relation as [25]

$$\frac{\tau_0}{\tau_{av}} = 1 + k_q^{TR}\tau_0[Q]_{eff} \quad (4)$$

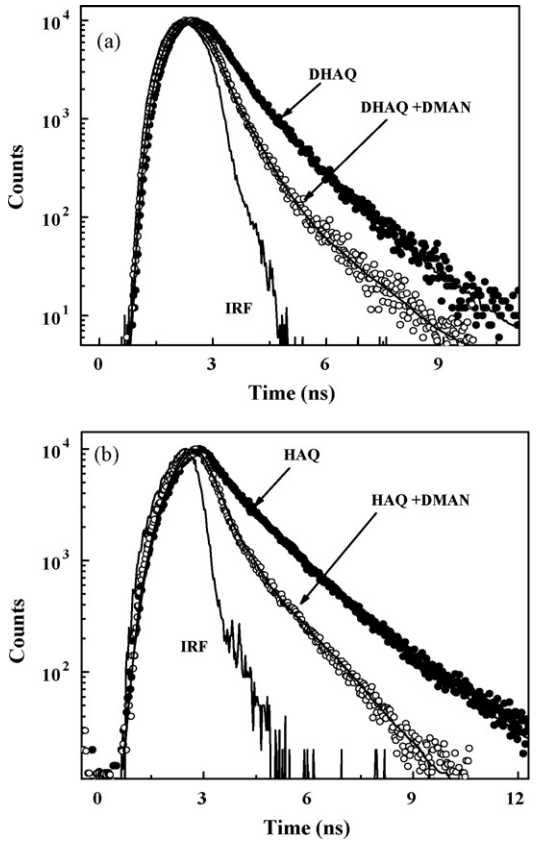

Fig. 2. (a) Fluorescence decays of DHAQ (with 560 nm excitation) in the absence (τ_0 = 0.69 ns) and in presence of DMAN ($[Q]_{eff}$ = 0.48 M; τ_1 = 0.18 ns (70%) and τ_2 = 0.60 ns (30%)) in CTAB micelle. (b) Fluorescence decays of HAQ (with 373 nm excitation) in the absence (τ_0 = 1.33 ns) and in presence of DMAN ($[Q]_{eff}$ = 0.50 M; τ_1 = 0.35 ns (73%) and τ_2 = 1.20 ns (27%)) in CTAB micelle. To be noted that DHAQ corresponds to the data point at the maxima and HAQ corresponds to the data point at the inversion region of the Marcus correlation curve shown in Fig. 3.

where τ_0 is the lifetime of the quinone in the absence of the quencher and $[Q]_{eff}$ is the effective quencher concentration in the corona region of the micelle. The $[Q]_{eff}$ values were estimated as discussed in Section 2. For the present systems, the τ_0/τ_{av} vs. $[Q]_{eff}$ plots were found to be linear up to the highest amine concentrations used (cf. Fig. 1(b)). The estimated quenching constants in TX100, BJ35 and CTAB micelles are listed in Tables 2–4, respectively. To be mentioned here that this approach of using τ_{av} to estimate an average quenching kinetics in micellar systems has been used extensively by many research groups [10–16,18–22,30]. In the present context, it is important to be mentioned that in micellar solutions there is a well-discussed quenching kinetic model reported in the literature [1,31,32], where, the quenchers are considered to migrate between the micellar and the aqueous phases, and the excited fluorophores are considered to undergo quenching by the quencher molecules with a unified quenching constant per quencher occupancy in the micelle. It has been shown in our earlier studies using coumarin–amine and quinone–amine systems that such a kinetic model does not give any satisfactory result for the observed TR quenching in micellar media involving ET process [11–16]. It has been argued that in micellar media since ET reaction takes place effectively without any lateral diffusion of the reactants, the above kinetic model becomes non-applicable for such ET systems. Accordingly, for bimolecular ET reactions in different micellar media we adopted the approach of using the bi-exponential analysis of the fluorescence decays to obtain an average picture of the TR fluorescence quenching and hence to estimate the average quenching constant, k_q^{TR}, as applied in the present cases. To be mentioned that for the similar quinone–amine systems in SDS micellar solution, we also applied this approach to estimate the effective quenching constant k_q^{TR} [13].

For quinone–amine systems, ET is supposed to be the likely mechanism for the observed fluorescence quenching [29,33,34], though a direct evidence for ET reaction could not be obtained in this study due to the non-availability of the transient absorption results. However, the ET mechanism in the present systems is strongly supported by the fact that an alternative singlet–singlet energy transfer mechanism is simply not feasible due to the lower

Table 3
Bimolecular quenching constants (k_q^{TR}, from TR measurements) and the free energy changes (ΔG°) for the ET reactions in quinone–amine systems in BJ35 micellar solution

Donor	Acceptor	τ_0 (ns)	ΔG° (eV)	k_q^{TR} ($\times 10^9$ dm^3 mol^{-1} s^{-1})
DMAN	AHAQ	0.89	−0.51	0.43
	DAAQ	0.69	−0.52	0.33
	DHAQ	2.22	−0.79	1.42
	HAQ	1.41	−1.49	0.62
DEAN	AHAQ		−0.53	0.29
	DAAQ		−0.54	0.51
	DHAQ		−0.81	0.96
	HAQ		−1.50	0.46
DMPT	AHAQ		−0.59	0.43
	DAAQ		−0.60	0.34
	DHAQ		−0.87	1.41
	HAQ		−1.57	0.60

Table 2
Bimolecular quenching constants (k_q^{TR}, from TR measurements) and the free energy changes (ΔG°) for the ET reactions in quinone–amine systems in TX100 micellar solution

Donor	Acceptor	τ_0 (ns)	ΔG° (eV)	k_q^{TR} ($\times 10^9$ dm^3 mol^{-1} s^{-1})
DMAN	AHAQ	0.88	−0.23	2.05
	DAAQ	0.69	−0.28	3.38
	DHAQ	0.68	−0.54	29.00
	HAQ	1.22	−1.23	16.06
DEAN	AHAQ		−0.27	2.46
	DAAQ		−0.32	5.74
	DHAQ		−0.58	32.52
	HAQ		−1.27	10.76
DMPT	AHAQ		−0.33	4.05
	DAAQ		−0.54	7.80
	DHAQ		−0.64	30.36
	HAQ		−1.33	11.90

Table 4
Bimolecular quenching constants (k_q^{TR}, from TR measurements) and the free energy changes (ΔG°) for the ET reactions in quinone–amine systems in CTAB micellar solution

Donor	Acceptor	τ_0 (ns)	ΔG° (eV)	k_q^{TR} ($\times 10^9$ dm^3 mol^{-1} s^{-1})
DMAN	AHAQ	0.93	−0.45	0.72
	DAAQ	0.71	−0.46	1.59
	DHAQ	0.69	−0.73	3.83
	HAQ	1.33	−1.50	1.97
DEAN	AHAQ		−0.47	1.19
	DAAQ		−0.49	2.12
	DHAQ		−0.75	3.58
	HAQ		−1.53	1.36
DMPT	AHAQ		−0.53	1.50
	DAAQ		−0.55	2.49
	DHAQ		−0.81	4.29
	HAQ		−1.58	1.78

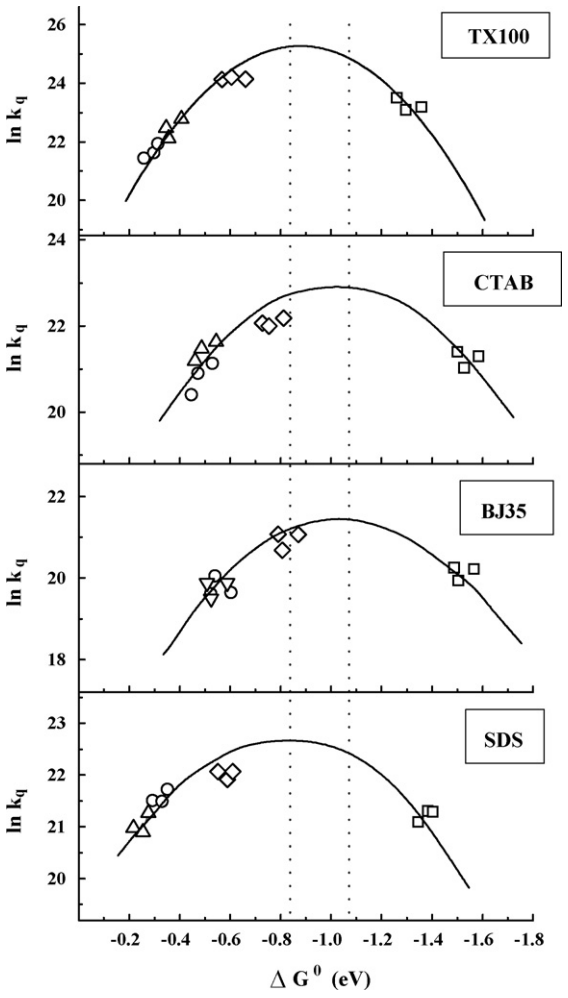

Fig. 3. The $\ln(k_q^{TR})$ vs. ΔG° plots for quinone–amine systems in different micelles. Experimental data are shown by symbols and continuous curves are drawn as the guide to the eyes to represent the trends. The symbols correspond to different acceptors are as HAQ (□), DHAQ (◊), AHAQ (○), and DAAQ (△).

S_1 state energies of quinones (E_{00}^q; cf. Table 1) than amines (E_{00}^{am}; cf. Table 1). Similarly a proton transfer mechanism has also been excluded for similar quinone–amine systems, because the k_q values do not show any correlation with the pK_b values of the amines as discussed in our earlier works [29,34].

The ΔG° values for the ET reactions in the present systems were calculated using Rehm–Weller relation [35] as

$$\Delta G^\circ = E\left(A/A^+\right) - E\left(Q/Q^-\right) - E_{00}^q - e^2/\varepsilon_s r_0 \quad (5)$$

where $E(A/A^+)$ and $E(Q/Q^-)$ are the oxidation and reduction potentials of amines and quinones, respectively, E_{00}^q is the excitation energy of the quinones in the S_1 state, e is the charge of an electron, ε_s is the static dielectric constant of the reaction medium, and r_0 is the center-to-center distance between the interacting quinone and amine molecules [35]. The ε_s values in the corona region was considered as 22, 28 and 37 for TX100, BJ35 and CTAB micelles, respectively [12,14,36]. Edward's volume addition method was used to calculate r_0 [37], assuming the reactants to be the effective spheres. The $E(A/A^+)$, $E(Q/Q^-)$, and E_{00}^q values for the present systems are given in Table 1 and the ΔG° and k_q^{TR} values in different micelles are listed in Tables 2–4. Fig. 3 shows the k_q^{TR} vs. ΔG° plots for the present quinone–amine systems in different micelles, where experimental data are shown by different symbols and the continuous curves are drawn as the guide to the eyes to represent the trends in the k_q^{TR} values with ΔG°. In all the cases, the presence of Marcus inversion is clearly evident. For a comparison, the previously reported Marcus plot for the same quinone–amine systems in SDS micelle [13] is also shown in Fig. 3.

As indicated from Fig. 3, the onset of Marcus inversion in SDS, TX100, CTAB and BJ35 micelles occurs at exergonicity values of 0.83, 0.87, 1.03 and 1.08 eV, respectively. Interestingly, these exergonicities appear to be always somewhat lower than the expected λ_s values in different micelles, as estimated following Eq. (6). Considering a dielectric continuum model for the solvent and assuming the reactants to be the effective spheres, λ_s can approximately be estimated using the following expression:

$$\lambda_s = e^2\left(\frac{1}{2r_D} + \frac{1}{2r_A} - \frac{1}{r_{eff}}\right)\left(\frac{1}{n^2} - \frac{1}{\varepsilon}\right) \quad (6)$$

where n is the refractive index, ε is the dielectric constant of the solvent (micellar corona region in the present case), r_D and r_A are the donor and acceptor radius, respectively and r_{eff} is the effective donor–acceptor separation for the interacting pair. Generally, r_{eff} is considered as the sum of donor and acceptor radii (donor–acceptor in contact), though in micellar ET, r_{eff} can be larger than donor–acceptor contact distance [14,25,28,38]. For simplicity, assuming r_{eff} as the donor–acceptor contact, the expected λ_s values in different micelles are estimated in the range of 1.11–1.15 eV. With higher r_{eff}, as may be the situation in real cases in micellar ET reactions, λ_s could be higher than the above estimates. Thus, it is evident that in the present systems the onset of Marcus inversion appears at lower exergonicity than expected from λ_s values. Such an observation can be rationalized using the concept of two-dimensional ET (2DET) theory [11–16,28,39]. In homogeneous solution where solvent relaxation is very fast, the reactant state (as well as product state) is always in its equilibrium configuration with respect to the solvent reorganization surrounding the reactants. For these systems conventional Marcus ET theory is well applicable to rationalize the observed ET dynamics. In cases where solvent relaxation is significantly slower, e.g. in micellar solution [11–16,40–46], it is expected that the ET reaction will effectively take place along the intramolecular coordinate (q) with a non-equilibrium configuration along the solvation coordinate (X), because solvent reorganization remains incomplete during the ET reaction, the basic concept of 2DET theory [39]. Thus, considering the 2DET theory for the present systems it is expected that only a fraction of λ_s will contribute to the free energy of activation $\Delta G^*(X)$ for the ET reaction, and will be given by the following equation [39,47]:

$$\Delta G^*(X) = \frac{\{\lambda_s(1-2X_g) + \Delta G^\circ + \lambda_i\}^2}{4\lambda_i} \quad (7)$$

where X_g is the nonequilibrium solvation coordinate for the reactant state. Due to this fractional contribution of λ_s towards $\Delta G^*(X)$, the onset of Marcus inversion occurs at a lower exergonicity than what it would have been in a medium where solvent relaxation is very fast such that X_g always becomes zero. Interesting to note from Fig. 3 that for the similar quinone–amine systems, the onset of Marcus inversion is shifted significantly along the exergonicity scale by ~0.25 eV, depending on the micelles used. Since solvent relaxation in different micelles is dependent on their micellar microenvironments and hydration characteristics, the fraction of λ_s that contribute to $\Delta G^*(X)$ also changes accordingly in different micelles. This in turn opens up the possibility of modifying/tuning the inversion region of the Marcus correlation curves for the ET reactions, might find its usefulness in different applied areas.

It is interesting to note from Fig. 3 that the Marcus correlation curves are apparently symmetric in nature for the present systems. It is reported in the literature [25,28,38] that Marcus correlation

Table 5
Different micellar parameters for TX100, BJ35, CTAB and SDS[a]

Micelles	CMC (mM)	N_{agg}	Micellar radius (Å)	Core radius (Å)	Volume per surfactant (Å^3)[b]	Free volume per surfactant chain (Å^3)[c]
TX100	0.24	100	50	25	627	4.61×10^3
BJ35	0.09	44	44	18	1148	6.96×10^3
CTAB	0.9	92	21.7	14.7	353	0.94×10^2
SDS	3.7	62	30	21	275	1.55×10^3

[a] Adopted from literature (Ref. [6,47–51]).
[b] Following Edwards's volume addition method (Ref. [37]).
[c] Obtained by subtracting the surfactant volume from the expected average volume per surfactant as estimated using micellar radius and its aggregation number. For ionic surfactants it is considered that around 60% of the micellar charge has been neutralized by the corresponding counter ions (Ref. [52]) and accordingly counter ion volume has also been considered. This excess volume can be available for the reactants (and also for the dissolved water and the counter ions).

curves often show asymmetric nature as a result of enhanced ET rates in the inversion region arising due to the involvement of high-frequency vibrational modes. For the present systems, since inversion region has been shifted significantly towards the lower exergonicity region due to the partial contribution of λ_s to $\Delta G^*(X)$ (cf. Eq. (7)), it is likely that the effect of high-frequency vibrational modes could be very nominal or negligible for the present systems [15]. A better realization of this aspect could be obtained if the range of reaction exergonicity was extended further in the inversion region. This is, however, beyond the scope of the present study.

For bimolecular ET reaction in homogeneous solution the translational diffusion of reactants is an important parameter as it determines the maximum bimolecular diffusional rate constant, k_d [25,28]. For most ET systems, even if the absolute ET rate is faster than the diffusional rate of the reactants, the effective rate constant can have its maximum value as k_d. In micellar solution, following fluorescence anisotropy measurements, it is possible to have an idea about the microviscosity of the reactant microenvironment and hence the expected k_d values. Using coumarin as the probes, it has been shown earlier that the expected k_d values in different micellar media should be in the range of $\sim 10^8$ mol^{-1} s^{-1} [11,14,16]. Since the observed k_q^{TR} values in the present systems are much higher than these k_d values in the micellar media, it is expected that bimolecular ET reaction in micelles takes place without any effective translational diffusion of the reactants. Accordingly, the distribution of the quenchers ($g(r)$) around an excited fluorophore that effectively determines the kinetics of the ET reaction, as discussed in relation to the bi-exponential analysis of the fluorescence decays.

Another interesting observation from Fig. 3 is that the k_q^{TR} values corresponding to the maxima of the Marcus correlation curves in different micelles vary by almost one order of magnitude. Even though the micro-polarity in different micelles has some role in the ET rates, the observation that the maximum k_q^{TR} value in the lower polarity TX100 micelle is higher than in the higher polarity SDS and CTAB micelles suggests that some other factor than simply the polarity that determines these differences in maximum k_q^{TR} values. The most expected reason for this observation is the differences in the effective electronic coupling parameter, V_{el}^{eff} [11,12,36], possibly arising due to the differences in the r_{eff} values of the interacting donor–acceptor pairs in different micelles. Since we deal with the same quinone–amine systems, differences in r_{eff} can only account for the differences in the V_{el}^{eff} values, as the later parameter is a function of r_{eff} as [28]

$$V_{el}^{eff} = V_{el}^{0} \exp\{-\beta(r_{eff} - r_0)\} \quad (8)$$

where V_{el}^{0} corresponds to the coupling parameter at donor–acceptor contact (r_0) and β is the attenuation coefficient. Considering, that the k_{et} (cf. Eq. (1)) and accordingly k_q^{TR} should change as a function of $(V_{el}^{eff})^2$, comparing the maximum k_q^{TR} values in different micelles, it is indicated that r_{eff} for the interacting quinone–amine pairs will gradually increase in the micelles TX100, SDS, CTAB and BJ35. These differences in the r_{eff} values in different micelles are possibly related to the compactness of the micellar microenvironments, though the later aspect is difficult to quantify in exact terms.

A qualitative idea about the free volume available for the reactants in a micelle can be obtained by subtracting the volume of the surfactants (estimated following Edward's method) from the available volume per surfactant in the micelle (obtained from the micellar radius and aggregation number) [6,48–52]. These free volumes are thus estimated to be ~6960 and ~4610 Å^3 for BJ35 and TX100 micelles, respectively (cf. Table 5). These values indicate that the reactants should be densely packed in TX100 than in BJ35 micelles, which corroborate at least qualitatively with the expected trend in the r_{eff} values in TX100 and BJ35 micelles. Also to be mentioned that the estimated rotational relaxation times for the fluorophores as obtained from fluorescence anisotropy measurements in TX100 are longer than that in BJ35 micelle, suggesting that the microenvironment in TX100 is more compact than in BJ35 [36].

The consideration of the free volume in the micelles as mentioned in the cases of TX100 and BJ35 micelles to rationalize the expected trends in the r_{eff} values (and in turn maximum k_q^{TR} values) seems not to be applicable in the cases of SDS and CTAB micelles. In these ionic micelles, nearly 60–70% charge neutralization occurs by the presence of counter ions in the corona region [52], which needs to be properly accounted while estimating the free volumes in these micelles. Additionally, the counter ion condensation is known to be greater in cationic micelle CTAB than in anionic micelle SDS. Therefore, it is difficult to envisage the correlation between free volumes and r_{eff} values in these ionic micelles.

Lastly, it should be mentioned here that, due to an increase in the reactant separation ($r_{eff} > r_0$), the actual λ_s values should be higher than what we considered earlier (λ_s in the range of 1.11–1.15 eV) for close-contact reactants. These alterations in the λ_s values can modify the curvature (stiffness) of the Marcus correlation curves as well as the onset of the Marcus inversion. Therefore, it is evident from Fig. 3 that only a fractional contribution of λ_s is in fact associated with the $\Delta G^*(X)$ values to bring the Marcus inversion at the lower exergonicities, as can be understood easily on the basis of the 2DET theory (cf. Eq. (7)). From the present results it is clearly indicated that there is a possibility of tuning the ET kinetics by changing the micellar environments, which can in turn modulate the exergonicity region of the Marcus inversion for an ET system.

4. Conclusions

The observed fluorescence quenching rates for quinone–amine ET systems in different micellar media show the Marcus inversion behavior on plotting reaction rates against ΔG° values. The results are rationalized on the basis of the 2DET theory, where ET is understood to occur along intramolecular coordinate, q, with only a fractional contribution of λ_s towards the free energy of

activation $\Delta G^{*}(X)$. It is observed that the onset of Marcus inversion is significantly shifted (~0.25 eV) along the exergonicity scale for different micelles used. This observation has been rationalized on the basis of the relative propensities of the ET and solvation rates in different micelles. Variations in the maximum k_q^{TR} values in different micelles are explained on the basis of the differences in the separations of the reactants which seem to be apparently related to the compactness of the micelles involved. Present results clearly indicate towards a possibility of tuning the Marcus inversion region for an ET system by changing the micellar microenvironments.

Acknowledgements

Authors are thankful to Dr. S.K. Sarkar, Head RPCD and Dr. T. Mukherjee, Director Chemistry Group, BARC, for their constant encouragement and support during the course of the present work.

References

[1] M. Tachiya, Can. J. Phys. 68 (1990) 797.
[2] Y.S. Kang, L. Kevan, J. Phys. Chem. 98 (1994) 2478.
[3] K. Weidemaier, M.D. Fayer, J. Phys. Chem. 100 (1996) 3767.
[4] K. Weidemaier, H.L. Tavernier, M.D. Fayer, J. Phys. Chem. B 101 (1997) 9352.
[5] H.L. Tavernier, A.V. Barzykin, M. Tachiya, M.D. Fayer, J. Phys. Chem. B 102 (1998) 6078.
[6] H.L. Tavernier, F. Laine, M.D. Fayer, J. Phys. Chem. A 105 (2001) 8944.
[7] I.V. Soboleva, J.v. Stam, G.B. Dutt, M.G. Kuzmin, F.C.D. Schryver, Langmuir 15 (1999) 6201.
[8] L. Chen, P.D. Wood, A. Mnyusiwalla, J. Marlinga, L.J. Johnston, J. Phys. Chem. B 105 (2001) 10927.
[9] S. Fukuzumi, M. Nishimine, K. Ohkubo, N.V. Tkachenko, H. Lemmetyinen, J. Phys. Chem. B 107 (2003) 12511.
[10] T.K. Mukherjee, P.P. Mishra, A. Datta, Chem. Phys. Lett. 407 (2005) 119.
[11] M. Kumbhakar, S. Nath, H. Pal, A.V. Sapre, T. Mukherjee, J. Chem. Phys. 119 (2003) 388.
[12] M. Kumbhakar, S. Nath, T. Mukherjee, H. Pal, J. Chem. Phys. 123 (2005) 034705.
[13] M. Kumbhakar, S. Nath, T. Mukherjee, H. Pal, J. Chem. Phys. 122 (2005) 084512.
[14] M. Kumbhakar, S. Nath, T. Mukherjee, H. Pal, J. Chem. Phys. 120 (2004) 2824.
[15] M. Kumbhakar, S. Nath, T. Mukherjee, H. Pal, J. Photochem. Photobiol. A: Chem. 182 (2006) 7.
[16] A.K. Satpati, M. Kumbhakar, S. Nath, H. Pal, J. Phys. Chem. B 111 (2007) 7550.
[17] M. Kumbhakar, P.K. Singh, S. Nath, A.C. Bhasikuttan, H. Pal, J. Phys. Chem. B 112 (2008) 6646.
[18] S. Ghosh, S.K. Mondal, K. Sahu, K. Bhattacharyya, J. Chem. Phys. 126 (2007) 204708.
[19] S. Ghosh, K. Sahu, S.K. Mondal, P. Sen, K. Bhattacharyya, J. Chem. Phys. 125 (2006) 054509.
[20] A. Chakraborty, D. Seth, P. Setua, N. Sarkar, J. Chem. Phys. 124 (2006) 074512.
[21] A. Chakraborty, D. Chakrabarty, P. Hazra, D. Seth, N. Sarkar, Chem. Phys. Lett. 382 (2003) 508.
[22] A. Chakraborty, D. Chakrabarty, P. Hazra, D. Seth, N. Sarkar, Chem. Phys. Lett. 387 (2004) 517.
[23] E. Vauthey, J. Phys. Chem. A 105 (2001) 340.
[24] S. Murata, M. Tachiya, J. Phys. Chem. A 111 (2007) 9240.
[25] J.R. Lakowicz, Principle of Fluorescence Spectroscopy, 3rd ed., Springer, New York, 2006.
[26] S. Nad, H. Pal, J. Phys. Chem. A 104 (2000) 673.
[27] M. Tachiya, S. Murata, J. Phys. Chem. 96 (1992) 8441.
[28] G.J. Kavarnos, Fundamentals of Photoinduced Electron Transfer, VCH Publishers, New York, 1993.
[29] H.N. Ghosh, H. Pal, D.K. Palit, T. Mukherjee, J.P. Mittal, J. Photochem. Photobiol. A 73 (1993) 17.
[30] S.K. Pal, D. Mandal, D. Sukul, K. Bhattacharyya, Chem. Phys. 249 (1999) 63.
[31] M. Tachiya, Chem. Phys. Lett. 33 (1975) 29.
[32] M. Tachiya, Kinetics of Non-Homogeneous Processes, Wiley, NY, 1987.
[33] S.M. Hubig, J.K. Kochi, J. Am. Chem. Soc. 121 (1999) 1688.
[34] M. Kumbhakar, S. Nath, M.C. Rath, T. Mukherjee, H. Pal, Photochem. Photobiol. 79 (2004) 1.
[35] D. Rehm, A. Weller, Israel J. Chem. 8 (1970) 259.
[36] M. Kumbhakar, T. Goel, T. Mukherjee, H. Pal, J. Phys. Chem. B 108 (2004) 19246.
[37] J.T. Edwards, J. Chem. Educ. 47 (1970) 261.
[38] P.F. Barbara, T.J. Meyer, M.A. Ratner, J. Phys. Chem. 100 (1996) 13148.
[39] H. Sumi, R.A. Marcus, J. Chem. Phys. 84 (1986) 4894.
[40] Y. Tamoto, H. Segawa, H. Shirota, Langmuir 21 (2005) 3757.
[41] A. Datta, D. Mandal, S.K. Pal, K. Bhattacharyya, J. Mol. Liq. 77 (1998) 121.
[42] N. Sarkar, A. Datta, S. Das, K. Bhattacharyya, J. Phys. Chem. 100 (1996) 15483.
[43] H. Shirota, Y. Tamoto, H. Segawa, J. Phys. Chem. A 108 (2004) 3244.
[44] K. Hara, H. Kuwabara, O. Kajimoto, J. Phys. Chem. A 105 (2001) 7174.
[45] D. Chakrabarty, P. Hazra, A. Chakraborty, N. Sarkar, Chem. Phys. Lett. 392 (2004) 340.
[46] D. Chakrabarty, A. Chakraborty, D. Seth, P. Hazra, N. Sarkar, J. Chem. Phys. 122 (2005) 184516.
[47] H. Shirota, H. Pal, K. Tominaga, K. Yoshihara, J. Phys. Chem. A 102 (1998) 3089.
[48] K. Streletzky, J.D. Philies, Langmuir 11 (1995) 42.
[49] S. Berr, R.R.M. Jones, J.J.S. Johnson, J. Phys. Chem. 96 (1992) 5611.
[50] J.D. Philies, R.H. Hunt, K. Strang, N. Sushkin, Langmuir 11 (1995) 3408.
[51] H.H. Paradies, J. Phys. Chem. 84 (1980) 599.
[52] K. Kalyansundaram, Photochemistry in Microheterogeneous Systems, Academic Press, Orlando, 1987.